INTERNATIONAL JOURNAL FOR NUMERICAL AND ANALYTICAL METHODS IN GEOMECHANICS
Int. J. Numer. Anal. Meth. Geomech., **24,** 183–199 (2000)

ELASTO-PLASTIC MODELLING OF STRESS-PATH-DEPENDENT BEHAVIOUR OF INTERFACES

KAZEM FAKHARIAN[1†] AND ERMAN EVGIN[2*‡]

[1] *Department of Civil Engineering, Amirkabir University of Technology, Tehran 15875, Iran*
[2] *Department of Civil Engineering, University of Ottawa, Ottawa, ON, Canada, K1N 6N5*

SUMMARY

A single-surface elasto-plastic model developed by Desai and his coworkers is used to predict the behaviour of an interface between sand and a steel plate. The loading in the experiments and in their predictions followed various stress and displacement paths. The results of predictions of the two- and three-dimensional behaviour of the interface under both constant normal stress and constant normal stiffness conditions are presented. The predictions are compared with their corresponding experimental results. The model parameters were determined on the basis of 2-D conventional experiments under the condition of constant normal stress and they were used in the prediction of the interface behaviour in various stress paths. There is, in general, a good agreement between the predicted and experimental results. Copyright © 2000 John Wiley & Sons, Ltd.

KEY WORDS: interface testing; elasto-plastic modelling; sand–steel interface; stress path; 3-D testing; constant normal stiffness

INTRODUCTION

The contact zone between two materials is normally referred to as an interface. The soil–structure interaction problems and the problems related to the mechanics of jointed rock involve interface behaviour. The response of soil–structure systems, such as shallow and deep foundations, lined tunnels, retaining walls, and reinforced earth, to monotonic and cyclic loads, is influenced by the characteristics of interfaces. The strength parameters and stress–displacement relations of interfaces play an important role on the load–deformation behaviour of such systems. Numerical analyses of these systems require reliable constitutive models for both interface and continuum bodies, which consist of soils and structural materials.

Various constitutive models have been developed for interfaces, such as Mohr–Coulomb-type models, non-linear elastic models,[1] a directional-type model,[2] and elasto-plastic models.[3–5] The general formulation of the elasto-plastic type models for interface behaviour is similar to that of the continuum materials. Ghaboussi and Wilson[3] applied a cap model to joints in rock. They used a perfectly plastic yield surface to limit shear stresses and a strain hardening cap to control

* Correspondence to: Dr. Erman Evgin, Department of Civil Engineering, University of Ottawa, Ottawa, Ontario, K1N 6N5, Canada. E-mail: eevgin@uottawa.ca

† Assistant Professor.
‡ Professor

CCC 0363–9061/2000/020183–17$17.50

Received 2 January 1997
Revised 28 August 1998; 6 May 1999

dilatancy. Desai and Ma[6] developed a model on the basis of the disturbed state concept. This recent model was formulated for use in both normal stress and normal stiffness controlled boundary conditions.

Fishman and Desai[4] and Desai and Fishman[7] developed an elasto-plastic constitutive model for the hardening behaviour of rock joints using associative and non-associative flow rules. The basic formulation of this model was the same as the one used for frictional materials by Desai,[8] Desai and Faruque,[9] and Desai *et al.*[10] The same model was modified by Navayogarajah[11] and Navayogarajah *et al.*[5] for monotonic and cyclic behaviour of interfaces between sand–steel and sand–concrete. The model was developed on the basis of the experimental results reported by Kishida and Uesugi,[12] Uesugi and Kishida,[13,14] and Uesugi *et al.*[15] The experimental results were obtained from a simple shear-type apparatus, which had the capability of separating interface sliding from the deformation of the soil mass. Separate measurements of interface sliding and soil deformation are not possible in interface experiments with a direct-shear-type apparatus.

A new Cyclic 3-Dimensional Simple Shear Interface (C3DSSI) apparatus was described by Fakharian and Evgin[16] and Evgin and Fakharian.[17] The apparatus was designed for testing interfaces between soils and structural materials.[18] A simple shear-type soil container is used in C3DSSI to distinguish between the sliding displacement at the interface and shear deformation of the soil mass. C3DSSI has the capability of 3-D loading of the interface. Two of these three loads lie in the plane of the interface and generate the required shear stresses. The third load is perpendicular to the interface plane and applies the normal stress. The apparatus is also capable of imposing a constant stiffness condition in the direction normal to the interface plane. An experimental program was undertaken on an interface between medium crushed Silica sand and a rough steel plate. Monotonic and cyclic, 2-D and 3-D, constant normal stress and constant normal stiffness tests were conducted following various stress and displacement paths including a rotational loading path.

The mathematical model by Navayogarajah *et al.*[5] was selected in this study to simulate the 3-D behaviour of interfaces as well as the behaviour of interfaces under various boundary conditions in the direction normal to the interface. This choice of the mathematical model was based on the following considerations:

(1) The model was formulated using the theory of plasticity, and thus has a strong theoretical basis.
(2) The model was developed using the experimental results from a simple shear-type apparatus. It is capable of simulating non-associativeness, strain softening, and the observed response in cyclic loading.

This paper presents (i) a review of the 3-D formulation of the model for monotonic loading, (ii) the technique used for the simulation of constant normal stiffness condition, and (iii) the comparisons between the model predictions and the experimental results published in Reference 18.

STRESSES AND DISPLACEMENTS

The stresses acting on 3-D and 2-D interfaces are illustrated in Figure 1. There are two shear stress components, τ_x and τ_y, and a normal stress, σ_n, acting on the 3-D interface which has a thickness of 't'. In the case of 2-D interfaces, there are only two stress components, i.e. σ_n and τ_x. A simple shear type soil container in C3DSSI allows the interface to be sheared in two orthogonal directions, i.e. along the x- and y-axis, simultaneously. A stack of 2 mm thick, anodized, Teflon

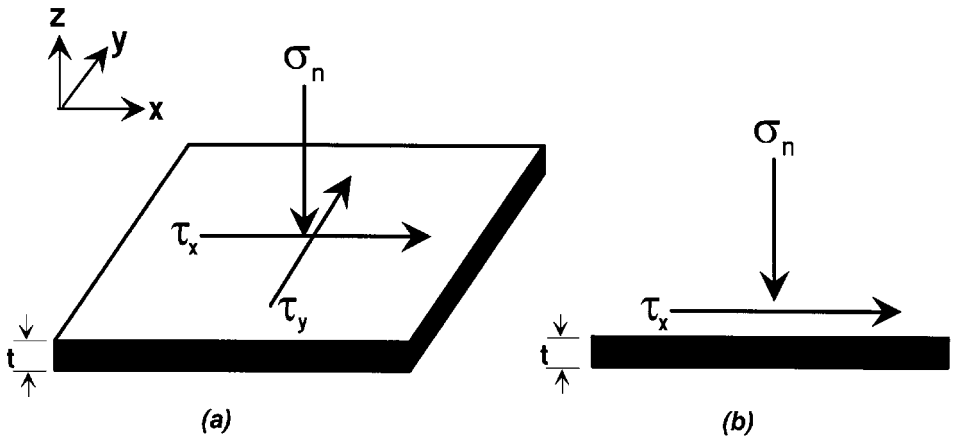

Figure 1. Stresses acting on an interface: (a) 3-D, (b) 2-D

coated, square aluminium plates with an inside area of 100 mm × 100 mm is placed on the steel plate which has an area of 300 mm × 300 mm (Figure 2). Two sets of tangential displacements are measured to distinguish between the sliding displacement (slip) along the contact surface and the shear deformation of the soil mass in both x- and y-directions. All displacements are measured by LVDTs. Figures 2(a) and 2(b) illustrate the schematic diagrams of tangential displacements in the x- and y-directions, respectively. In the x-direction, the total tangential displacement, u_{xa}, is measured by the LVDT, a_x, which reads the difference in displacements between the top aluminium plate and the steel specimen. The displacement resulting from the shear deformation of the soil mass, u_{xb}, is measured by the LVDT, b_x, which reads the relative tangential displacement between the top and bottom aluminum plates. The sliding displacement at the soil–steel interface, u_x, is obtained from $u_x = u_{xa} - u_{xb}$ (Figure 2(a)).

In the y-direction, the total tangential displacement, u_{ya}, is measured by the LVDT, a_y, which reads the relative displacement between the top aluminium plate and the steel specimen. The displacement resulting from the shear deformation of the soil mass, u_{yb}, is measured by the LVDT, b_y, which reads the relative tangential displacement between the top and bottom aluminium plates. The sliding displacement at the soil–steel interface, u_y, is obtained from $u_y = u_{ya} - u_{yb}$ (Figure 2(b)).

For modelling purposes, the sliding displacements, u_x and u_y, are used as the tangential displacement components. The normal displacement, v, results from the deformations in the normal direction both in the interface layer and in the sand mass.

The degree of roughness of a surface is usually defined using the surface profile which is obtained from the intersection of the surface with a plane normal to the surface. The maximum peak-to-valley height, $R_{\max}$, proposed by DIN standard, is used here to give a measure of the surface roughness as illustrated in Figure 3. The sampling length (gauge length), L, was set as 0·8 mm on the surface roughness tester device which was the closest to the D_{50} of the sands used in this study. The sands used in this study had $D_{50}s$ of 0·6 mm and 1·2 mm. The construction material was a 300 × 300 mm low carbon steel plate. Sand blasting technique was used to create the rough surfaces for the tests requiring higher surface roughness. A new steel plate was used for every test to ensure that $R_{\max}$ is constant in all experiments.

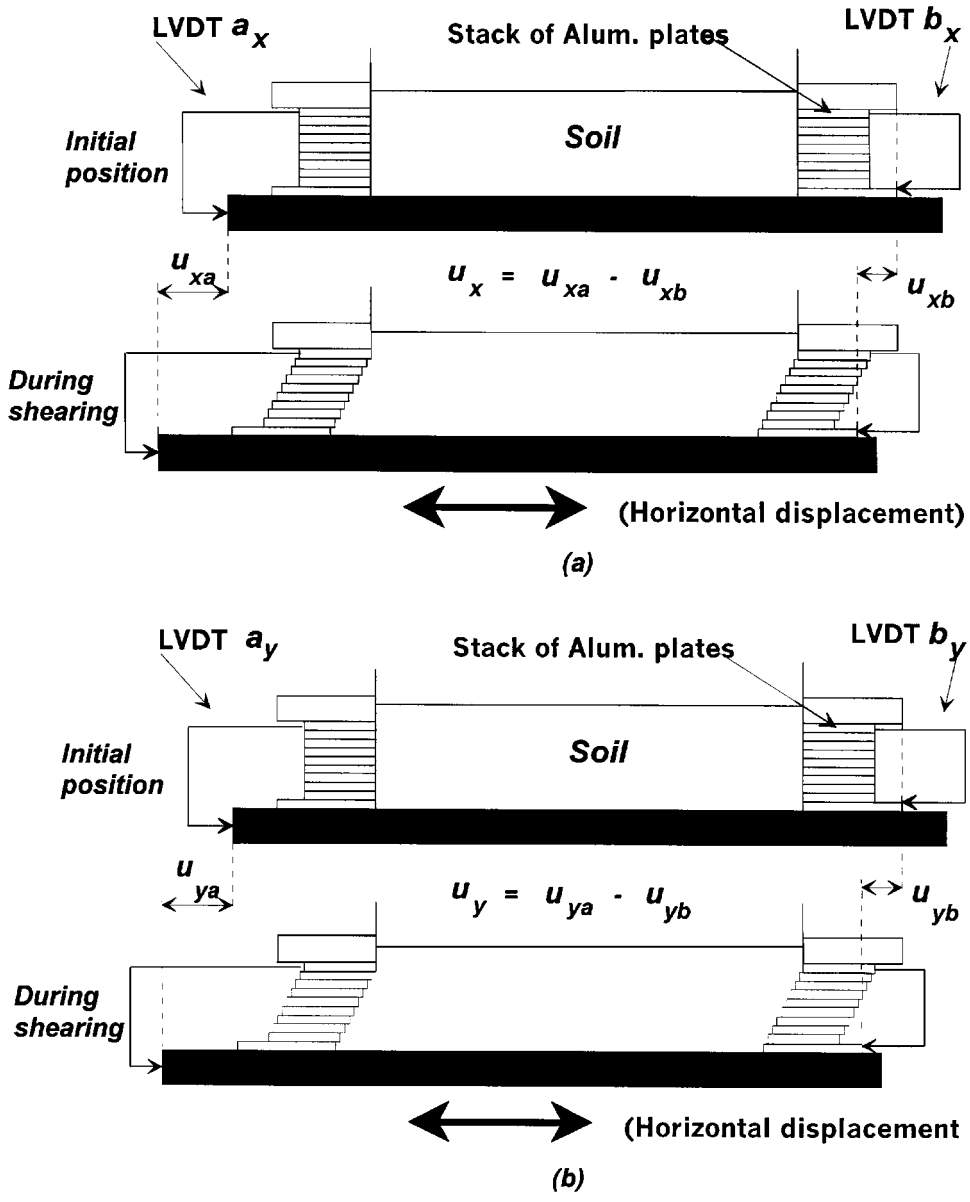

Figure 2. Schematic diagrams of shear displacements: (a) x-direction, (b) y-direction

DESCRIPTION OF THE MODEL

The constitutive relation of interface behaviour relates the increments of normal and shear stresses ($d\sigma_n$, $d\tau_x$, and $d\tau_y$) to the increments of normal and tangential displacements

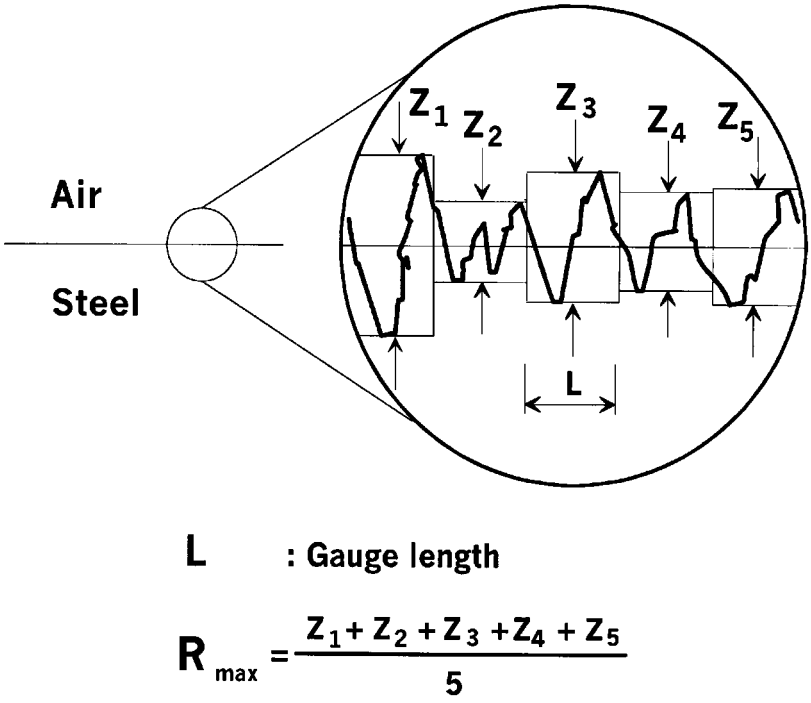

Figure 3. Illustration of surface roughness, $R_{\max}$

(dv, du_x, and du_y) written as

$$\mathrm{d}\sigma = C^{\mathrm{ep}}\mathrm{d}U \tag{1}$$

where $\mathrm{d}\sigma^{\mathrm{T}} = (\mathrm{d}\sigma_n, \mathrm{d}\tau_x, \mathrm{d}\tau_y,)$; $\mathrm{d}U^{\mathrm{T}} = (\mathrm{d}v, \mathrm{d}u_x, \mathrm{d}u_y)$; and C^{ep} is the elasto-plastic constitutive matrix (3×3 for 3-D interfaces and 2×2 for 2-D interfaces). The elasto-plastic matrix, $[C^{\mathrm{ep}}]$ is obtained from the following equation:

$$\begin{aligned}
[C^{\mathrm{ep}}] &= [C^{\mathrm{e}}] - [C^{\mathrm{p}}] \\
&= \begin{bmatrix} K_n & 0 & 0 \\ 0 & K_{\mathrm{sx}} & 0 \\ 0 & 0 & K_{\mathrm{sy}} \end{bmatrix} - \begin{bmatrix} C^{\mathrm{p}}_{11} & C^{\mathrm{p}}_{12} & C^{\mathrm{p}}_{13} \\ C^{\mathrm{p}}_{21} & C^{\mathrm{p}}_{22} & C^{\mathrm{p}}_{23} \\ C^{\mathrm{p}}_{31} & C^{\mathrm{p}}_{32} & C^{\mathrm{p}}_{33} \end{bmatrix} \\
&= \begin{bmatrix} K_n - C^{\mathrm{p}}_{11} & -C^{\mathrm{p}}_{12} & -C^{\mathrm{p}}_{13} \\ -C^{\mathrm{p}}_{21} & K_{\mathrm{sx}} - C^{\mathrm{p}}_{22} & -C^{\mathrm{p}}_{23} \\ -C^{\mathrm{p}}_{31} & -C^{\mathrm{p}}_{32} & K_{\mathrm{sy}} - C^{\mathrm{p}}_{33} \end{bmatrix}.
\end{aligned} \tag{2}$$

In equation (2), C^{e} is the elastic constitutive matrix, C^{p} is the plastic constitutive matrix, K_n, K_{sx} and K_{sy} are the elastic normal stiffness in the z-direction, the shear stiffness in the x-direction, and the shear stiffness in the y-direction, respectively. It is assumed that the elastic normal and

shear behaviour is uncoupled. For this simulation of the test results in this study, it is assumed that

$$K_{sx} = K_{sy} \tag{3}$$

C_{ij}^{p} represents the components of the plastic constitutive matrix.

The relationship between the elastic displacement increments and stress increments is

$$\{dU^{e}\} = [C^{e}]^{-1}\{d\sigma\} \tag{4}$$

The plastic components of displacements can be obtained as

$$\{dU^{p}\} = \{dU\} - \{dU^{e}\} \tag{5}$$

YIELD SURFACE

Desai,[8] Desai and Faruque,[9] and Desai *et al.*[10] proposed a general 3-D yield function written in terms of stress invariants:

$$F = J_{2D} - \left(\frac{-\alpha J_1}{\alpha_0} + \gamma J_1^2\right)(1 - \beta S_r)^m = J_{2D} - F_b F_s = 0 \tag{6}$$

where J_1 is the first invariant of the stress tensor and J_{2D} is the second invariant of the deviatoric stress tensor S_{ij}. The parameters α, γ, β, and m are the response functions, and S_r equals stress ratio such as $J_{3D}^{1/3}/J_{2D}^{1/2}$, where J_{3D} is the third invariant of S_{ij}. F_b and F_s are referred to as the basic and shape functions and are related to the shape of F in $J_1 - \sqrt{J_{2D}}$ stress space.

Using the analogies between the behaviour of soils and interfaces, equation (6) was specialized for 2-D interfaces by Fishman and Desai (1987):

$$F = \tau^2 + \alpha\sigma_n^n - \gamma\sigma_n^2 = 0 \tag{7}$$

In this equation, the symbols γ and n are the interface parameters; and α is a hardening function that defines the evolution of the yield surface during deformation. To simulate the occurrence of the peak shear stress (τ_p) at small shear displacements, the following relation was proposed for α by Navayogarajah *et al.*:[5]

$$\alpha = \gamma \exp(-a\xi_v)\left(\frac{\xi_D^* - \xi_D}{\xi_D^*}\right)^b \quad \text{for } \xi_D < \xi_D^*$$
$$\alpha = 0 \quad \text{for } \xi_D \geqslant \xi_D^* \tag{8}$$

The parameter γ is related to the ultimate (or failure) condition; a and b are some additional interface parameters; $\xi_v = \int |dv^p|$ and $\xi_D = \int |du^p|$ are the plastic volumetric and shear displacement trajectories, respectively. ξ_D^* becomes equal to ξ_D when τ reaches τ_p. It was found that ξ_D^* was predominantly a function of the parameter R which was defined as

$$R = \begin{cases} R_n/R_n^{cri} & \text{if } R_n^{cri} > R_n \\ 1 & \text{if } R_n^{cri} \leqslant R_n \end{cases} \tag{9}$$

where R_n is the normalized roughness:

$$R_n = \frac{R_{\max}(L = D_{50})}{D_{50}} \tag{10}$$

and R_n^{cri} is the critical normalized roughness beyond which shear failure occurs in soil rather than at the interface. Numerically, R varies from 0 to 1, and it is a non-dimensional quantity.

Based on the experimental evidence, the parameters τ_{p} and ξ_{D}^* were related to R as

$$\mu_{\text{p}} = \frac{\tau_{\text{p}}}{\sigma} = \frac{1}{\bar{R}}\left[\mu_{\text{p1}} + \mu_{\text{p2}} R\right] \tag{11}$$

$$\gamma = \mu_{\text{p}}^2$$

$$\xi_{\text{D}}^* = (\xi_{\text{D1}}^* + \xi_{\text{D2}}^* R) \tag{12}$$

Here, μ_{p} is the ultimate (or peak) stress ratio, $\bar{R}$ denotes the roundness of sand particles, and μ_{p1}, μ_{p2}, ξ_{D1}^*, and ξ_{D2}^* are interface parameters.

Desai and Ma[6] and Navayogarajah *et al.*[5] adopted the concept of decomposition of material behaviour to model the strain-softening behaviour of interfaces. The observed or average response of an interface was assumed to be the sum of two parts, namely: (1) the Relative Intact (RI) part; and (2) the Fully Adjusted (FA) part, which can represent the damaged part. During the shear loading, the RI part is progressively transformed into the FA part due to the accumulation of plastic strains. The characterization of the RI and FA parts is achieved by using the theories of elasto-plasticity and rigid plasticity, respectively. The non-associative model is used for the RI part. It is assumed that the shear strength of the FA part is zero, but it can sustain normal stress. The normal stress is assumed to be compressive. With these assumptions, the observed or average interface stresses τ and σ_n can be written as

$$\begin{Bmatrix} \sigma_n \\ \tau \end{Bmatrix} = (1 - r) \begin{Bmatrix} \sigma_n^t \\ \tau^t \end{Bmatrix} + r \begin{Bmatrix} \sigma_n^t \\ 0 \end{Bmatrix} \tag{13}$$

The parameter $r = (A_0/A)$ is a scalar quantifying the damage, A_0 is the area of FA part, and A is the total area. The state of stress vectors $\{\sigma_n, \tau\}$, $\{\sigma_n^t, \tau^t\}$, and $\{\sigma_n^t, 0\}$, relate to average, RI part, and FA part of the interface, respectively.

The following relation was proposed for the damage function r:

$$r = 0 \quad \text{for } \xi_{\text{D}} < \xi_{\text{D}}^*$$

$$r = r_u - r_u \exp\left[-A(\xi_{\text{D}} - \xi_{\text{D}}^*)^2\right] \quad \text{for } \xi_{\text{D}} \geqslant \xi_{\text{D}}^* \tag{14}$$

where

$$r_u = \frac{\tau_{\text{p}} - \tau_r}{\tau_{\text{p}}} \tag{15}$$

A is a parameter that depends on the roughness ratio R of the interface. The residual stress ratio, μ_0, is related to R as

$$\mu_0 = \frac{\tau_r}{\sigma_n} = \frac{1}{\bar{R}}\left[\mu_{01} + \mu_{02} R\right] \tag{16}$$

Here, μ_{01} and μ_{02} are interface parameters.

For the case of 3-D interface elements, J_{2D} is

$$J_{2D} = \tfrac{1}{6}\left[(\sigma_{11} - \sigma_{22})^2 + (\sigma_{22} - \sigma_{33})^2 + (\sigma_{11} - \sigma_{33})^2\right] + \sigma_{12}^2 + \sigma_{23}^2 + \sigma_{13}^2 \tag{17}$$

and

$$\sigma_{33} = \sigma_n$$

$$\sigma_{13} = \tau_x$$

$$\sigma_{23} = \tau_y$$

$$\sigma_{11} = \sigma_{22} = \sigma_{12} = 0$$

Therefore,

$$J_{2D} = \tfrac{1}{3}\sigma_n^2 + \tau_x^2 + \tau_y^2 \tag{18}$$

The yield surface described by equation (7) can be written as

$$F = \tau_x^2 + \tau_y^2 + \alpha\sigma_n^n - \gamma\sigma_n^2 = 0 \tag{19}$$

The non-associative flow rule and the formulation for the strain-softening behaviour are used exactly in the same manner as Navayogarajah *et al.*[5]

2-D CONSTANT NORMAL STRESS TESTS

The predictions for 2-D monotonic tests on sand-steel interface are presented together with the corresponding experimental results in Figure 4. The predictions were made for an interface between medium Silica sand at a relative density of 88 per cent and steel plates with surface roughness of 4, 15, and 25 μm, which cover a range from very smooth to rough. The experimental results are only available for surface roughness of 4 and 25 μm. The normal stress was 100 kPa in all cases presented in this group. The determination of the parameters is described in Reference 18 and their values are shown in Table I. The model requires 12 parameters. The parameters were obtained using the results of 2-D monotonic tests under constant normal stress conditions. The test results presented in Figure 4 and various other test results related to coarse Silica sand were utilized for the determination of the parameters. These parameters were then used to predict the test results related to different loading or boundary conditions such as the 3-D loading and the constant normal stiffness condition as will be presented in the subsequent sections.

The predictions shown in Figure 4 seem to be in good agreement with the experimental results. The shear stress-sliding displacement results indicate that both peak and residual stresses are predicted adequately. Most of the model parameters are dependent on the interface roughness ratio, R. Therefore, the effect of surface roughness on peak and residual strengths are well captured in the predictions. The dilative response of the interface is also well predicted by the model, however, the compressive mode is not simulated well. For example, Figure 4(b) shows that for smooth surfaces the predicted normal displacement is zero whereas the experimental results show compression. Similarly, the initial compression portion for the rough surface is not predicted. The compressive mode is controlled by the phase change parameter n. Compression occurs in the soil mass in the vicinity of the interface, and the dilation is the result of particle

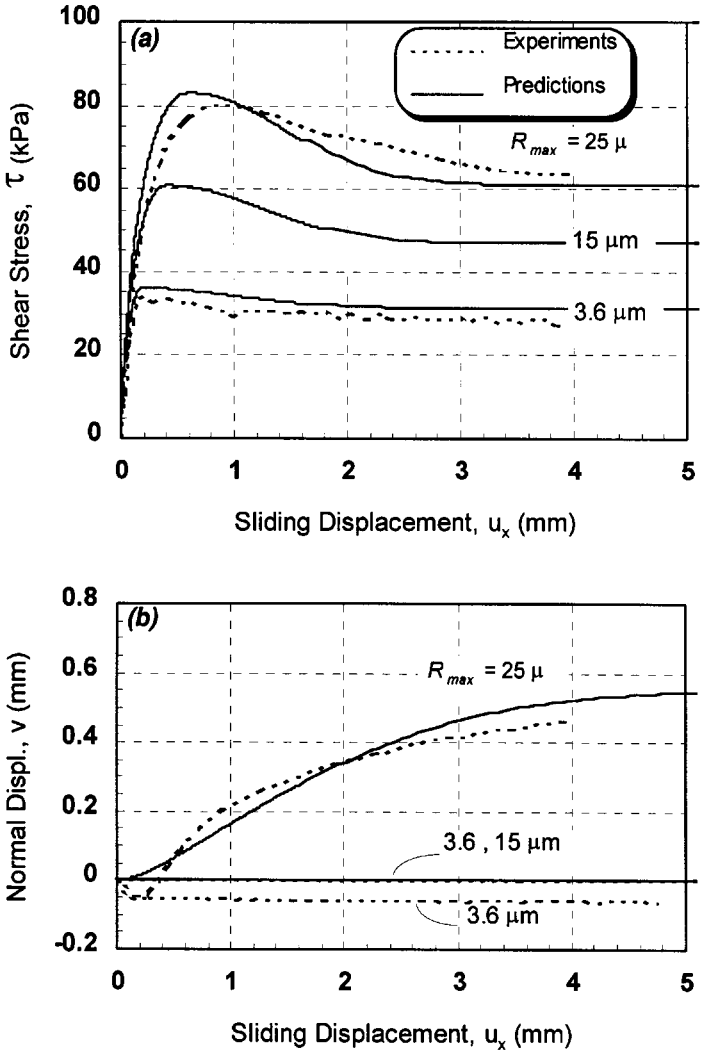

Figure 4. Comparison between *predicted* and *experimental* results for various roughnesses: 2-D constant normal stress Surface: Steel plate ($R_{\max} = 25$, 15 (predicted only), and 3·6 μm for $L = 0{\cdot}8$ mm) Sand: Medium Silica, $D_r = 88$ per cent; $\sigma_n = 100$ kPa

movements in the interface in the direction normal to the interface plane. Therefore, Navayogarajah[11] concluded that interface cannot undergo compression, but it can dilate or remain in steady state condition during monotonic loading. In such a case the shear stress at the phase change point, τ_{ph}, is very small or equal to zero leading to a value $n = 2{\cdot}0$. Navayogarajah adopted a value of 2·001 for n.

Table I. Model parameters

Model parameters		Toyoura sand–steel Navayogarajah (1990)	Silica sand–steel (this study)
(1)	(2)	$\sigma_n = 98$ kPa $D_r = 90\%$	$\sigma_n = 100$ kPa $D_r = 88\%$
R_n^{cri}	—	0·184	0·053
γ	μ_{p1}	0·081	0·275
—	μ_{p2}	0·1509	0·695
n	—	2·001	2·005
ξ_D^* (mm)	ξ_{D1}^*	0·035	0·09
—	ξ_{D2}^*	0·1679	0·559
a	—	20·5	22·5
b	—	1·5	2·2
κ	κ_1	− 1·94	− 1·26
—	κ_2	0·97	0·63
r_u	μ_{o1}	0·0648	0·257
—	μ_{o2}	0·1167	0·443
A	—	2·0	0·5
K_n	—	80000 kPa/mm	6000
K_s	—	4000 kPa/mm	1000

3-D CONSTANT NORMAL STRESS TESTS

Predictions were made for the results of the 3-D monotonic tests using the constitutive model. These tests were carried out under a constant normal stress of 100 kPa.[17] The parameters obtained from the 2-D test results, as presented in Table I, were used subsequently in all predictions without modification. The procedure followed in the 3-D experiments is as follows: A shear stress was applied first in the y-direction up to a target value. In the four experiments described in this section, the target values were 0, 20, 40, and 60 kPa. Subsequently, the interface was sheared in the x-direction while the normal stress in the z-direction and the shear stress in the y-direction were maintained at their specified values. This procedure was followed exactly for the tests with target values of 0, 20, and 40 kPa. When the target value τ_y was 60 kPa, the loading steps were the same as in the other tests up to the peak strength value. After the peak strength was reached, in this particular test, the values of both τ_x and τ_y reduced and the resultant shear stress moved toward the residual strength envelope. The reason why this type of behaviour was observed in one of the experiments was explained in Evgin and Fakharian.[17]

The comparisons between the predictions and the experimental results are presented in Figures 5 and 6. The computational steps for the predictions followed the loading steps in the experiments. The initial normal stress was specified as 100 kPa. Initially, shear stresses, τ_x and τ_y, were zero. Subsequently, shear stress increments in the y-direction, $\Delta\tau_y$, were applied while the shear stress in the x-direction, τ_x, remained at zero. The shear stress, τ_y, was increased until it reached its target value. After this step, $\Delta\tau_y$ was zero and the tangential displacement increments in the x-direction, Δu_x were specified for tests with τ_y equal to 0, 20, and 40 kPa. For the predictions of the test results where τ_y was equal to 60 kPa up to the peak strength and reduced thereafter, the loading path followed in the predictions was identical to that in the experiment.

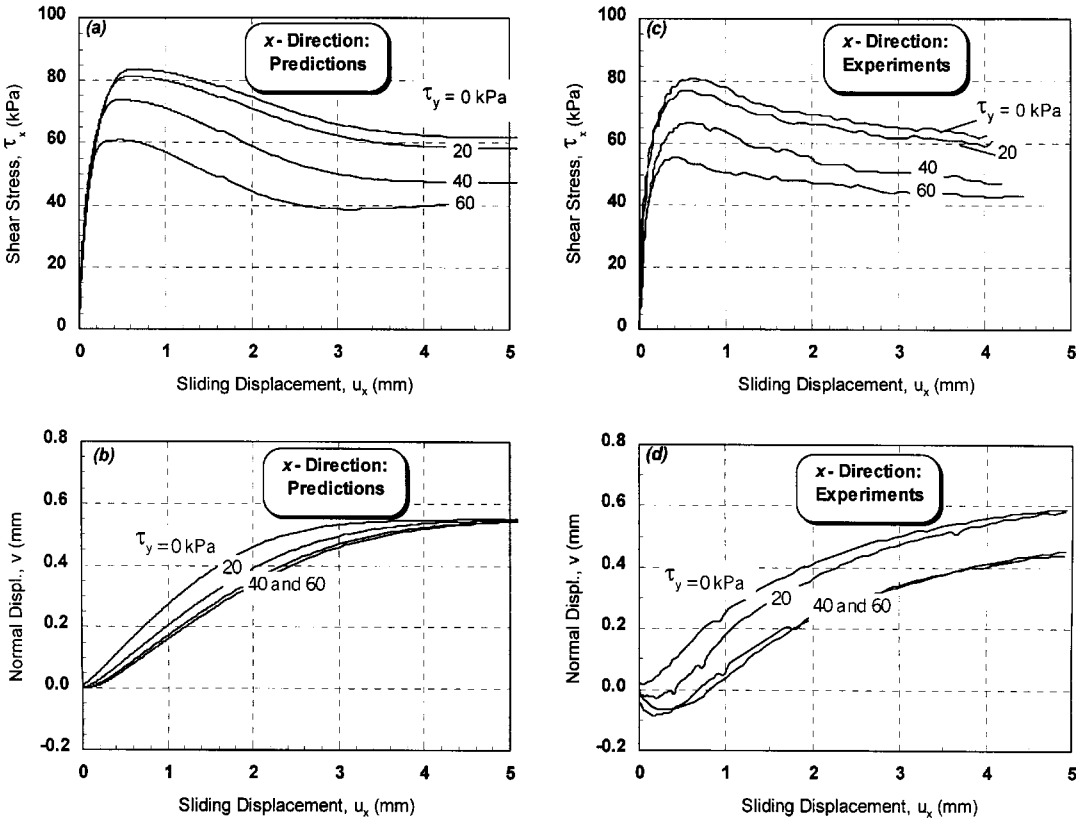

Figure 5. Comparison between *predicted* and *experimental* results for various values of τ_y: 3-D constant normal stress; $\sigma_n = 100$ kPa; $\tau_y = 0$, 20, 40, 60 kPa Surface: Steel plate ($R_{max} = 25$ μm for $L = 0{\cdot}8$ mm) Sand: Medium Silica, $D_r = 88$ per cent

Figure 6 shows that although only the shear stress, τ_x, was changing after the specified τ_y was reached, both the sliding displacement and the shear deformation of sand had components in the y-direction as well as in the x-direction. This type of response is different than the response of an elastic material that would deform in the x-direction alone. The simultaneous changes in both shear strain components with any change in one of the shear stresses are clear indications of the importance of three-dimensional testing and the 3-D modelling of interface behaviour. A more detailed explanation of such effects is provided in Evgin and Fakharian.[17]

Comparisons between the curves shown in Figures 5(a) and 5(c) indicate that the peak strength in the x-direction is slightly over estimated in all predictions. As the sliding displacement increased after the peak strength, strain softening took place in all cases. The strength reduction from the peak values to the residual values, however, was faster in the predictions than in the experiments. The predictions and the experimental data for the normal displacement variations with the sliding displacement, u_x, compare reasonably well as demonstrated in Figures 5(b) and 5(d).

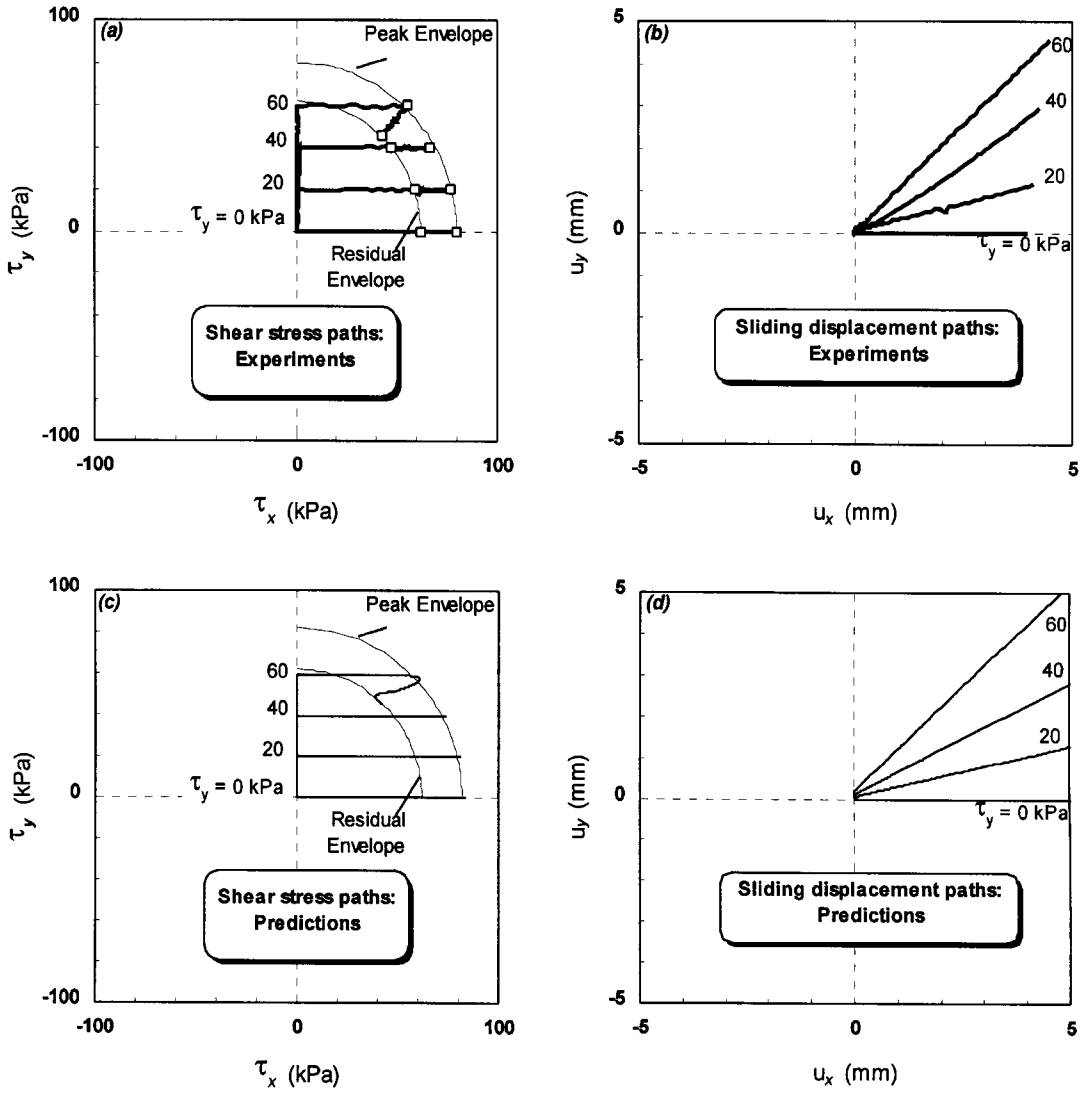

Figure 6. Comparison between stress and displacement paths for *predicted* and *experimental* results: 3-D constant normal stress; $\sigma_n = 100$ kPa; $\tau_y = 0$, 20, 40, 60 kPa

The shear stress paths and sliding displacement paths are illustrated in Figure 6. It should be noted that, the shearing in the y-direction was stress controlled whereas it was displacement controlled in the x-direction. All shear stress paths in both experiments and predictions are identical. The sliding displacement paths are also in very good agreement. These results illustrate how well this elasto-plastic model simulates the coupling effects between the shear stress and the tangential displacements on the x–y plane.

The comparisons presented so far showed that the model is capable of capturing the important aspects of the interface behaviour between sand and steel.

2-D CONSTANT NORMAL STIFFNESS CONDITION

The stiffness in the direction normal to the interface is usually denoted by K and it is defined as the ratio of the variation in the normal stress to the variation in the normal displacement at the top boundary of the sample, i.e. $K = \mathrm{d}\sigma_n/\mathrm{d}v$. Three typical boundary conditions (Figure 7) are generally used in laboratory experiments:

Case I: $K = 0$, i.e. $\mathrm{d}\sigma_n = 0$; $\mathrm{d}v \neq 0$ (constant normal stress).

Case II: $K = \infty$, i.e. $\mathrm{d}\sigma_n = 0$; $\mathrm{d}v = 0$ (constant volume).

Case III: $K =$ Constant, i.e. $\mathrm{d}\sigma_n \neq 0$; $\mathrm{d}v \neq 0$ and $\mathrm{d}\sigma_n/\mathrm{d}v = K$ (constant normal stiffness).

Case I represents the condition in which the normal stress does not change during the process of shearing as shown in Figure 7(a). In this case, the interface may compress or dilate freely ($\mathrm{d}\sigma_n = 0$; $\mathrm{d}v \neq 0$). The constant normal stress condition is the simplest and the most frequently employed boundary condition in interface experiments.

Case II is the condition of constant volume. No displacement is allowed at the top boundary of the sample in the direction normal to the interface plane as illustrated in Figure 7(b). During the test, the normal stress increases or decreases depending on the tendency of the soil to dilate or compress ($\mathrm{d}\sigma_n \neq 0$; $\mathrm{d}v = 0$).

Case III is the condition of constant normal stiffness (Figure 7(c)) in which normal stress and normal displacement vary proportionally ($\mathrm{d}\sigma_n/\mathrm{d}v = K$). Cases I and II are the lower and upper bounds of Case III, respectively.

The application of such boundary conditions in the described elasto-plastic model is as follows:

The constitutive equation is

$$\{\mathrm{d}\sigma\} = [C^{\mathrm{ep}}]\{\mathrm{d}U\} \tag{20}$$

or

$$\{\mathrm{d}U\} = [D^{\mathrm{ep}}]\{\mathrm{d}\sigma\} \tag{21}$$

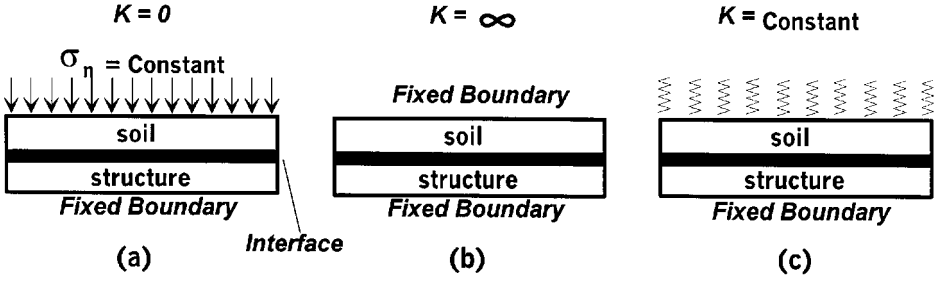

Figure 7. Boundary conditions in the direction normal to the interface: (a) constant normal stress, (b) constant volume, (c) constant normal stiffness

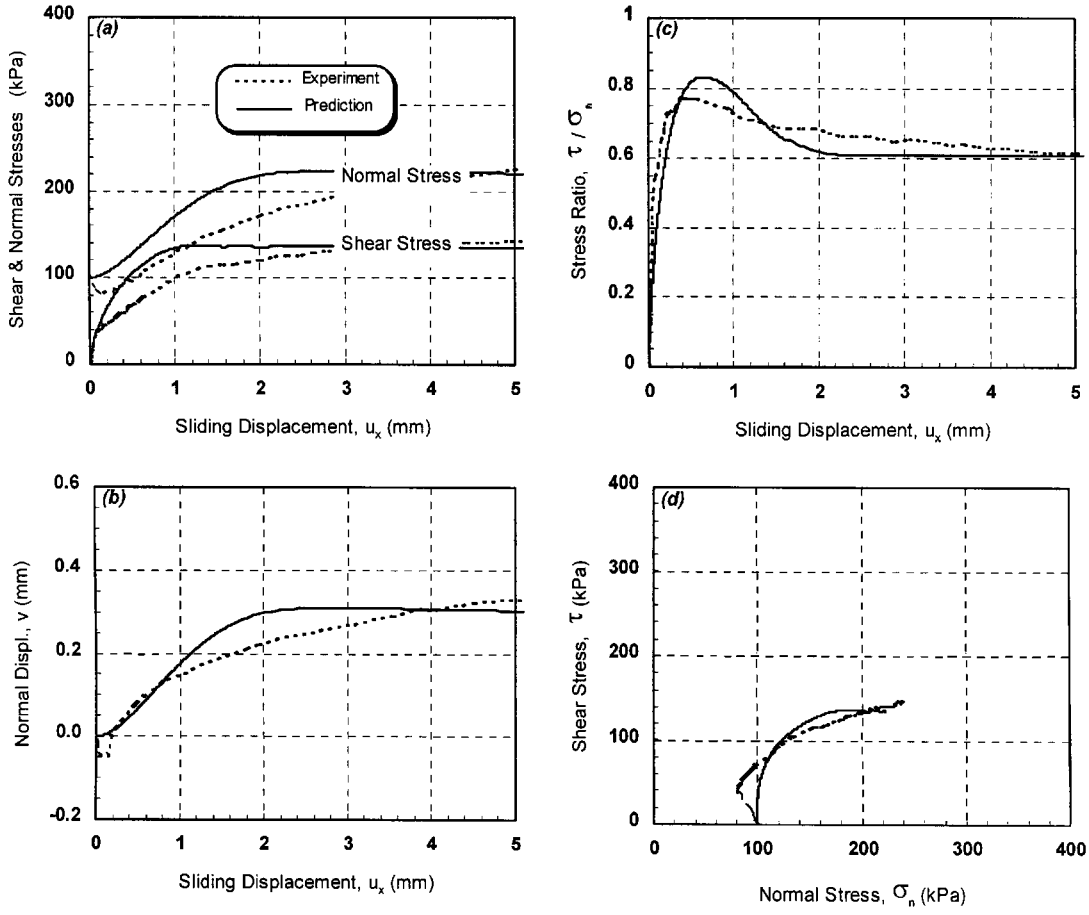

Figure 8. Comparison between *predicted* and *experimental* results for 2-D constant normal *stiffness*: $K = 400$ kPa; $\sigma_{n0} = 100$ kPa. Surface: Steel plate ($R_{max} = 25$ μm for $L = 0{\cdot}8$ mm) Sand: Medium Silica, $D_r = 88$ per cent

where

$$[D^{ep}] = [C^{ep}]^{-1} \tag{22}$$

Expanding equation (21) for the 2-D case gives

$$\begin{aligned} dv &= D_{11}^{ep}\, d\sigma_n + D_{12}^{ep}\, d\tau \\ du &= D_{21}^{ep}\, d\sigma_n + D_{22}^{ep}\, d\tau \end{aligned} \tag{23}$$

When these two equations are used to make predictions for the constant normal stress tests, $d\sigma_n$ is input as zero. For the prediction of the constant volume tests, dv is set equal to zero. In the case of constant normal stiffness conditions, $d\sigma_n$ in equation (23) can be substituted in each increment by $K_n\, dv$ and then the linear equations are solved. This technique is used to predict the results of constant normal stiffness experiments given in Reference 17. The results of three predictions are compared with the corresponding experimental results, as illustrated in Figures 8–10. In the experiments, the normal stiffness was kept constant at 400, 800, and 1200 kPa/mm in

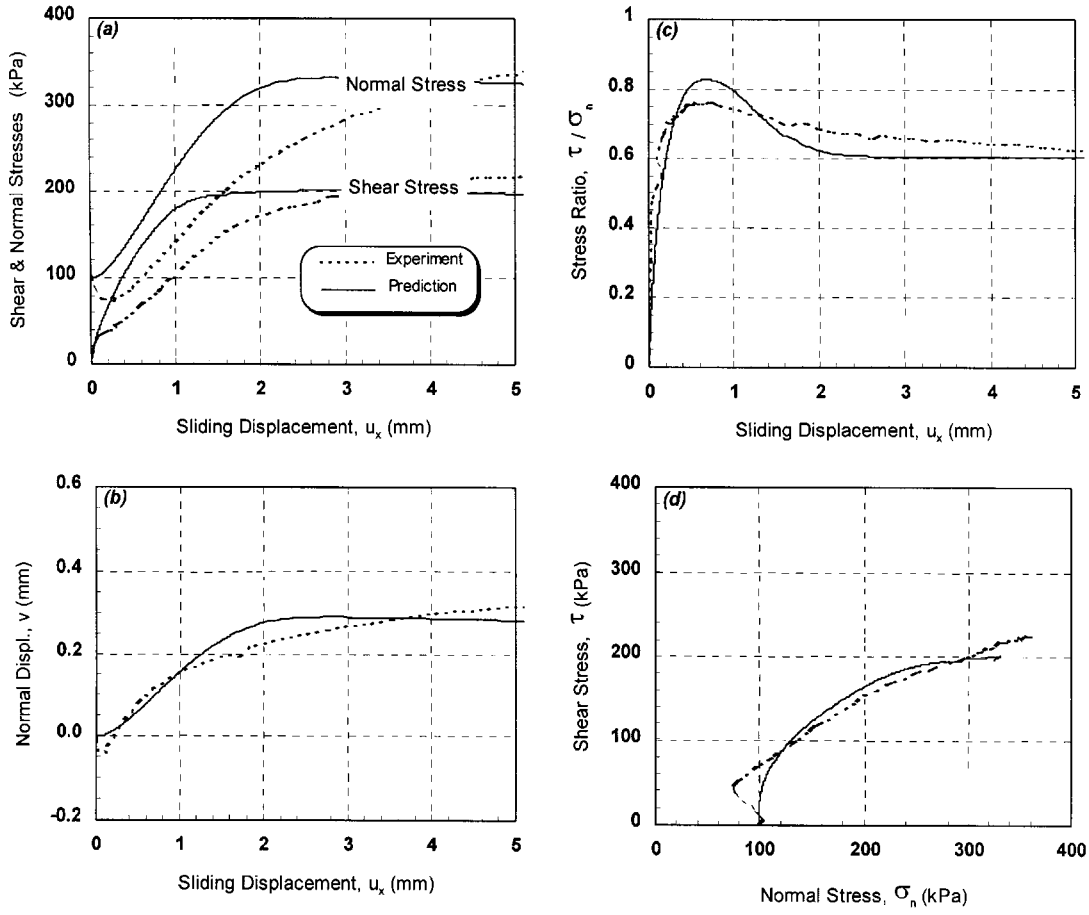

Figure 9. Comparison between *predicted* and *experimental* results for 2-D constant normal *stiffness*: $K = 800$ kPa; $\sigma_{n0} = 100$ kPa

these three tests. The initial normal stress was 100 kPa. The parameters listed in Table I were used for the predictions. These parameters were the same as those used for the prediction of 2-D monotonic test results under constant stress condition.

The predicted results are qualitatively in good agreement with the experimental results. There are some discrepancies in the peak strength ratios such that the predictions are about 15 per cent less than the measured values. This is attributed to the fact that the model does not incorporate the effect of the normal stress on the peak strength. The predicted peak strength ratios are the same as those in the constant normal stress test results. However, the experiments give lower values because of the increase in normal stress during shearing. In order to simulate this type of behaviour, γ should be expressed as a function of σ_n. The magnitude of the mobilized shear stress and the increase in normal stress are generally predicted well. Based on these results, it can be stated that the model is capable of simulating the behaviour of interfaces under various boundary conditions and stress paths.

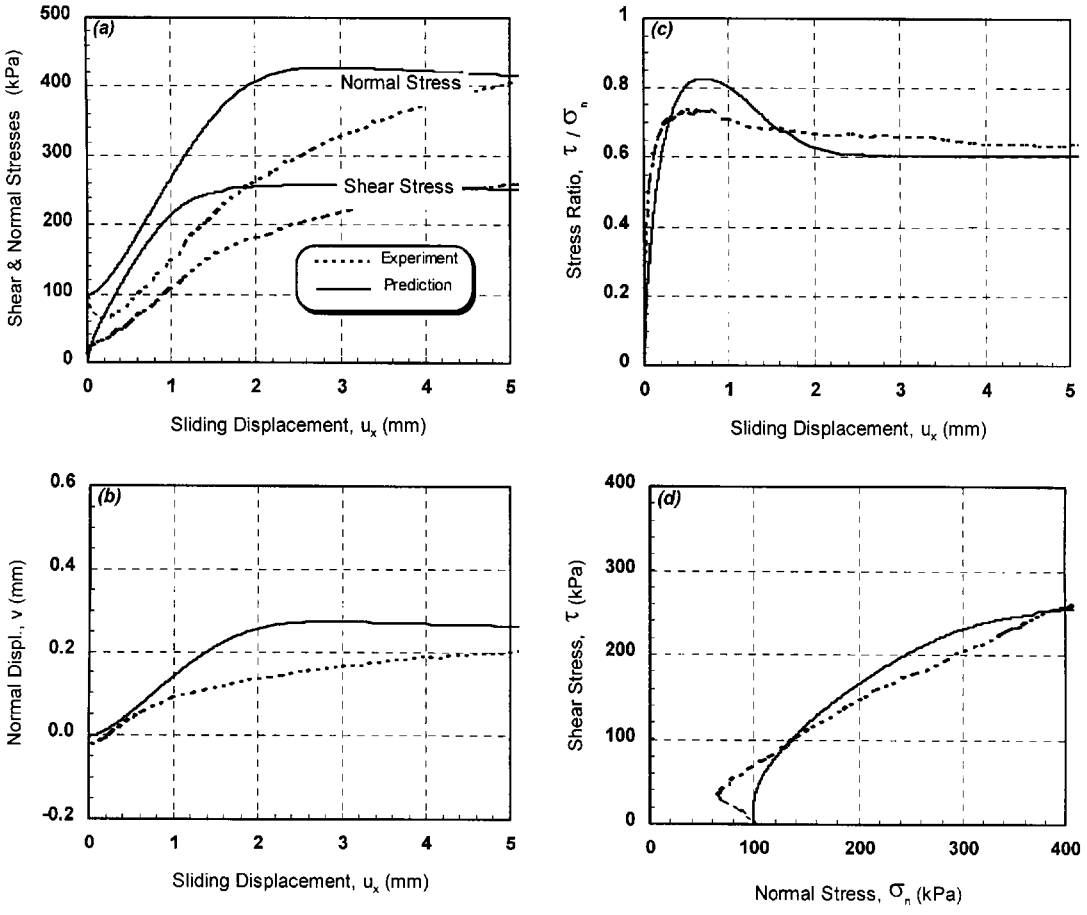

Figure 10. Comparison between *predicted* and *experimental* results for 2-D constant normal *stiffness*: $K = 1200$ kPa; $\sigma_{n0} = 100$ kPa

CONCLUSIONS

An elasto-plastic single-surface constitutive model developed by Desai and his coworkers[5] is used in this study to predict the behaviour of sand–steel interfaces. The model is known to be capable of predicting strain-softening and non-associative behaviour of interfaces. In this study, the formulation of the model is expressed in 3-D stress space. Predictions were made for four tests and the results were presented together with the corresponding experimental data. A special method was used in the calculations to simulate the constant normal stiffness condition. The effect of the magnitude of the constant normal stiffness on the interface behaviour was shown. The conclusions of this study are as follows:

(1) The peak and residual strengths are adequately predicted in all stress paths.
(2) The model is capable of simulating the dilative response of the interface. However, it needs some improvement to predict the compressive response of interfaces.

(3) The model needs some improvement to incorporate the effect of the magnitude of normal stress on the interface behaviour under the condition of constant normal stiffness. The general trend of the stress–displacement behaviour of interfaces is, however, well captured by the model.

REFERENCES

1. C. S. Desai, E. C. Drumm and M. M. Zaman, 'Cyclic testing and modeling of interfaces', *J. Geotech. Engng.* ASCE, **111**(6), 793–815 (1985).
2. M. Boulon and C. Plytas, 'Soil structure directionally dependent interface constitutive equations—application to the prediction of shaft friction along piles', *Proc. 2nd Int. Symp. on Numerical Models in Geomechanics*, 1986, pp. 43–54.
3. J. Ghaboussi and E. L. Wilson, 'Finite element for rock joints and interfaces', *J. Soil Mech. Foundations Div.*, ASCE, **99**(SM10), 833–848 (1973).
4. K. L. Fishman and C. S. Desai, 'A constitutive model for hardening behaviour of rock joints'. in Desai *et al.* (eds), *Constitutive Laws for Engineering Materials*: *Theory and Applications*, 1987, pp. 1043–1050.
5. N. Navayogarajah, C. S. Desai and P. D. Kiousis, 'Hierarchical single-surface model for static and cyclic behaviour of interfaces', *J. Engng. Mech.* ASCE, **118**(5), 990–1011 (1992).
6. C. S. Desai and Y. Ma, 'Modeling of joints and interfaces using the disturbed state concept', *Int. J. Numer. Anal. Meth. Geomech.* **16,** 623–653 (1992).
7. C. S. Desai and K. L. Fishman, 'Plasticity-based constitutive model with associated testing for joints', *Int. J. Rock Mech. Min. Sci.*, **28**(1), 15–26 (1991).
8. C. S. Desai, 'A general basis for yield, failure and potential functions in plasticity', *Int. J. Numer. Anal. Meth. Geomech.*, **4,** 361–375 (1980).
9. C. S. Desai and M. O. Faruque, 'Constitutive model for (geological) materials', *J. Engng. Mech. Div.*, ASCE **110** (1984).
10. C. S. Desai, S. Somasundaram and G. Frantziskonis, 'A hierarchical approach for constitutive modelling of geological materials', *Int. J. Numer. Anal. Meth. Geomech.*, **10,** 225–257 (1986).
11. N. Navayogarajah (1990).
12. H. Kishida and M. Uesugi, 'Tests of interface between sand and steel in the simple shear apparatus', *Geotechnique*, **37**(1), 45–52 (1987).
13. M. Uesugi and H. Kishida, 'Influential factors between steel and dry sand', *Soils Found.*, **26**(2), 33–46 (1986*a*).
14. M. Uesugi and H. Kishida, 'Frictional resistance at yield between dry sand and mild steel', *Soils Found.*, **26**(4), 139–149 (1986*b*).
15. M. Uesugi, A. H. Kishida and Y. Tsubakihara, 'Behaviour of sand particles in sand-steel friction', *Soils Found.*, **28**(1), 107–118 (1988).
16. K. Fakharian and E. Evgin, 'An automated apparatus for three-dimensional monotonic and cyclic testing of interfaces', *Geotech. Testing J.* ASTM, **19**(1), 22–31 (1996).
17. E. Evgin and K. Fakharian, 'Effect of stress paths on the behaviour of sand–steel interfaces', *Can. Geotech. J.*, **33**(6), 853–865 (1996).
18. K. Fakharian, 'Three-dimensional monotonic and cyclic behaviour of sand–steel interfaces: testing and modelling', *Ph.D. Thesis*, Department of Civil Engineering, University of Ottawa, Ottawa, Ontario, Canada, 1996.

